Azbel'-Kaner Cycoltron Resonance in Mercury*†

A. E. DIXON
Department of Physics, University of Waterloo, Waterloo, Ontario, and Department of Physics, McMaster University, Hamilton, Ontario‡
AND
W. R. DATARS§
Department of Physics, McMaster University, Hamilton, Ontario
(Received 24 June 1968)

Azbel'-Kaner cyclotron resonance in single-crystal mercury was studied at 1.2°K with frequencies of 35 and 70 GHz, using the slightly curved free surface of the mercury crystals as the sample surface. Cyclotron effective-mass results from four samples with different crystal orientations are reported and interpreted using Keeton and Loucks's relativistic augmented-plane-wave model of the Fermi surface. Cyclotron resonance from three orbits with minimum-mass values $0.63m_0$ (α orbit), $0.16m_0$ (β orbit), and $0.72m_0$ (τ orbit) are identified. The effective mass of the γ orbit is $0.69m_0$ with the magnetic field along the binary direction. The ratio of the measured cyclotron-mass values to that predicted by the single-orthogonalized-plane-wave approximation is 1.75 ± 0.1. Quantum oscillations of the microwave surface impedance from orbits on the β arms of the Fermi surface are reported.

I. INTRODUCTION

LITTLE information about the Fermi surface of mercury was available before 1965, although anomalous skin effect results had been reported,[1] and de Haas–van Alphen effect measurements had been made on unoriented crystals[2] and on crystals oriented using their magnetic anisotropy.[3] A positron-annihilation experiment[4] had been completed on liquid and solid mercury. Recently, both experimental and theoretical results have provided considerable information. The topology and size of several sections of the Fermi surface have been measured using the de Haas–van Alphen effect,[5] and magnetoresistance measurements[6,7] have indicated the direction and angular range of magnetic field for which open orbits exist. The relativistic augmented-plane-wave (RAPW) method has been used to calculate the electronic band structure of mercury, and to predict the shape of the Fermi surface.[8] Mercury can be obtained commercially in a very pure form, which made it feasible to attempt a cyclotron-resonance experiment, after the difficulties of growing single crystals with good surfaces were overcome. Mercury freezes at −38.9°C, and the single crystals are shiny and soft. In order to get good crystal surfaces, it was decided to use the free surface at the top of the crystal as the sample surface, even though that surface was curved rather than flat. The samples obtained in this way had smooth, extremely shiny surfaces, which gave large cyclotron-resonance signals. The signal shapes were slightly distorted, a property that has been attributed to the curved sample surface. Initial results of this experiment, as well as those of a magnetoresistance experiment, have been reported previously.[9]

Since electrons spiral about the direction of a constant magnetic field with a frequency equal to the cyclotron frequency, it is possible to cause resonance with a microwave field of suitable frequency. In metals the carrier density is so high that the microwave field only penetrates to a depth of the order of the classical skin depth, a distance typically 100 times smaller than the orbit diameter of the spiralling electrons. The suitable experimental geometry was first suggested by Azbel' and Kaner[10] in 1956. The sample is mounted so that it forms one wall of a microwave cavity, with a constant magnetic field parallel to the sample surface. The carriers spiralling in and out of the skin depth resonate with the microwave electric field if they return to the skin depth at the same point in an rf period during each cycle of their rotation. Consequently, resonance occurs whenever $\omega_c=\omega/n$, where ω is the applied rf frequency and n is an integer. If the microwave frequency is held constant and the magnetic field is slowly changed, cyclotron-resonance signals occur for $H_c=m_c^*c\omega/e$ and for $H=H_c/n$, where m_c^* is the extremal cyclotron effective mass. The cyclotron effective mass is related to the Fermi surface by

$$m_c^*=(\hbar^2/2\pi)\partial A/\partial E,$$

where A is the area of the orbit in $\mathbf{k}$ space in the plane normal to $\mathbf{H}$.

* Work supported by the National Research Council of Canada.
† This paper is based in part on a thesis submitted by one of the authors (A.E.D.) to McMaster University in partial fulfilment of the requirements for the Ph.D. degree in physics.
‡ Present address: Department of Physics, University of Waterloo, Waterloo, Ontario.
§ E.W.R. Steacie Fellow.
[1] A. B. Pippard, Proc. Roy. Soc. (London) **A191**, 385 (1947).
[2] B. I. Verkin, B. G. Lazarev, and N. S. Rudenko, Dokl. Akad. Nauk SSSR **80**, 45 (1951).
[3] D. Shoenberg, Phil. Trans. Roy. Soc. (London) **A245**, 1 (1952).
[4] D. R. Gustafson, A. R. Mackintosh, and D. J. Zaffarano, Phys. Rev. **130**, 1455 (1963).
[5] G. B. Brandt and J. A. Rayne, Phys. Rev. **148**, 644 (1966).
[6] W. R. Datars and A. E. Dixon, Phys. Rev. **154**, 576 (1967).
[7] J. H. Dishman and J. A. Rayne, Phys. Rev. **166**, 723 (1968).
[8] S. C. Keeton and T. L. Loucks, Phys. Rev. **152**, 548 (1966).
[9] A. E. Dixon and W. R. Datars, Solid State Commun. **3**, 377 (1965).
[10] M. Ya. Azbel' and E. A. Kaner, Zh. Eksperim. i Teor. Fiz. **30**, 811 (1956) [English transl.: Soviet Phys.—JETP **3**, 772 (1956)].

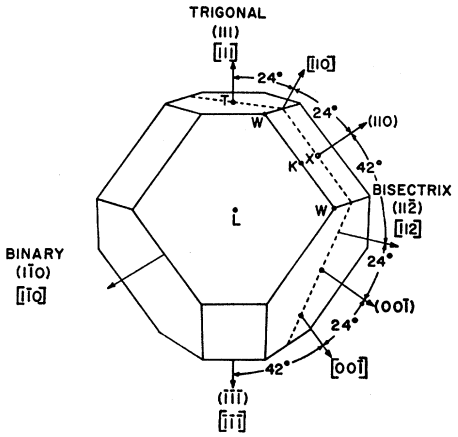

FIG. 1. First Brillouin zone of mercury and certain crystallographic directions.

The experiment was carried out to identify the groups of electrons on the Fermi surface that contribute to a resonance signal, to compare the results from these orbits with the predictions of a single-[orthogonalized-plane-wave (OPW)] Fermi surface and the Fermi surface predicted by the RAPW method,[8] to measure the cyclotron effective-mass values, and to estimate the mass enhancement due to electron-phonon and electron-electron interactions. The Fermi surface of mercury as predicted by both the single-OPW and RAPW models is described in Sec. II; a description of some possible closed orbits on the mercury Fermi surface is included, along with a summary of the pertinent results from de Haas–van Alphen effect and magnetoresistance experiments. The experimental apparatus and techniques are described in Sec. III. Section IV includes description and interpretation of the cyclotron-resonance results. Results obtained from quantum oscillations of the microwave surface impedance are described in Sec. V. Section VI includes a discussion of the effects of the curved sample surface on the cyclotron-resonance signals, a least-squares fit to compare the electron lenses with an ellipsoid of revolution, and a cylindrical fit to the quantum-oscillation data. The conclusions are summarized in Sec. VII.

II. FERMI SURFACE OF MERCURY

Mercury is a divalent atom, which crystallizes in a trigonal lattice, with one atom per unit cell. Thus the first Billouin zone, which can hold a maximum of two electrons, has the same volume as the free-electron Fermi sphere. At 5°K, the lattice constant of mercury has been measured to be 2.9963 Å, with a rhombohedral angle of 70° 44.6′.[11] An angle of 60° corresponds to an fcc lattice. The Brillouin zone was constructed following Jones,[12] and is shown in Fig. 1.

[11] C. S. Barrett, Acta Cryst. **10**, 58 (1957).

[12] H. Jones, *The Theory of Brillouin Zones and Electronic States in Crystals* (North-Holland Publishing Co., Amsterdam, 1960), p. 58.

It is necessary to be careful in converting directions in real space to directions in reciprocal space, because mercury is a noncubic crystal. The following convention is used. A direction in the crystal lattice is specified by $[lmn]$. A reciprocal lattice vector is designated (lmn), and is perpendicular to the set of planes (lmn) in the direct lattice. The orientation of a direction in real space with respect to the Brillouin zone is determined by finding the normal to the plane in reciprocal space containing all the reciprocal lattice vectors whose dot product with $[lmn]$ vanishes. The three orthogonal directions, trigonal, binary, and bisectrix, are specified by [111], [1$\bar{1}$0], and [11$\bar{2}$] in real space and by the same indices, (111), (1$\bar{1}$0), and (11$\bar{2}$), in reciprocal space. A set of equivalent directions in real space will be designated $\langle lmn\rangle$, and $\{lmn\}$ represents a set of equivalent planes in real space, or a set of equivalent reciprocal lattice vectors.

A model of the Fermi surface has been constructed using the single-OPW approximation described by Harrison.[13] This approximation is the same as the free-electron approximation except that there are connectivity modifications at the zone faces. The cyclotron effective mass of an orbit in this approximation is simply the total angle through which the electron moves divided by 2π, since the effective mass of an electron going around a sphere without reflections is unity.

The free-electron Fermi sphere cuts through the six L faces of the Brillouin zone, but does not quite touch the T or X faces (single-OPW approximation). This results in electron lenses in the second zone, and a first-zone hole surface composed of multiply connected tubes that will support open orbits in both the {100} and binary directions. A model of the first-zone hole surface is shown in Fig. 2(a). The model is oriented such that the dotted line drawn on the Brillouin zone of Fig. 1 would be drawn straight down the front of the model. Black areas on the model are areas where the surface is joined to other parts of the extended-zone surfaces. The model was constructed on a framework the size of the first Brillouin zone, and fills a volume of reciprocal space approximately twice that of one Brillouin zone. The single-OPW Fermi surface supports four closed orbits: around the second-zone electron lenses, a bow-tie-shaped hole orbit across the narrow dimension of the X faces, a hole orbit across the T faces starting at W and going across to the opposite corner, and a six-sided hole orbit in the trigonal plane centered at T. This orbit is slightly larger than the T face.

The RAPW calculation by Keeton and Loucks[8] predicts that the Fermi surface touches the zone boundary at the center of both the T and X faces, as shown in Fig. 3. Several closed orbits are possible in this model. Some of these orbits are shown in Fig. 2(b), where the areas of contact with the zone boundary are shown as a small circle on the T face and as rectangles

[13] W. A. Harrison, Phys. Rev. **118**, 1190 (1960).

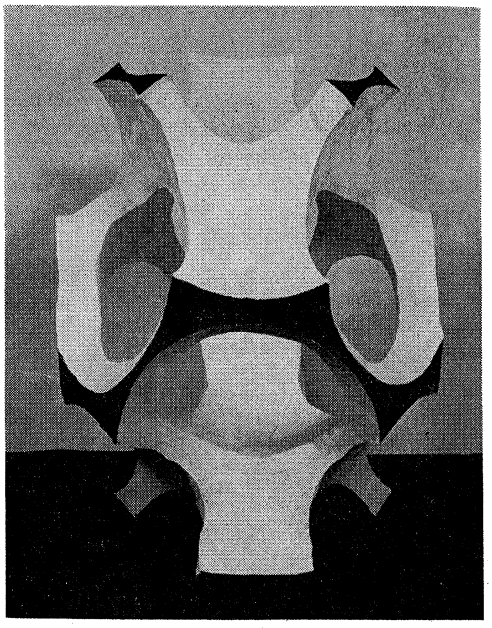

(a)

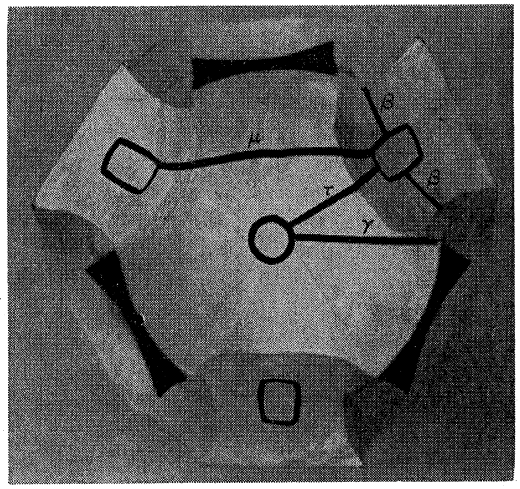

(b)

FIG. 2. (a) Model of the first-zone single-OPW surface of mercury. (b) Some of the closed orbits possible if the Fermi surface touches the zone boundary at the center of the T and X faces of the Brillouin zone.

with rounded corners on the X faces. The orbits are named to correspond with the convention used by Brandt and Rayne[5] and by Keeton and Loucks.[8] Some possible closed cyclotron orbits predicted by this model are the following [see Fig. 2(b)]:

α—an electron orbit around the second-zone lenses. It will be possible to see this orbit for any orientation of the magnetic-field direction with respect to the crystal axes.

T-face neck—an electron orbit around the neck where the Fermi surface touches the T faces. This orbit will be seen when the magnetic field is aligned accurately along the trigonal direction.

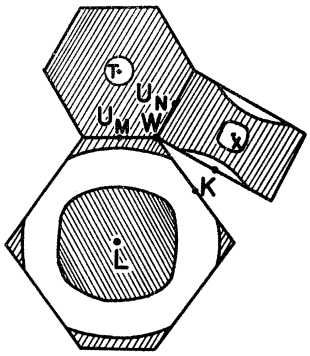

FIG. 3. Intersections of the Keeton-Loucks model of the Fermi surface of mercury with the Brillouin-zone faces.

X-face neck—an electron orbit around the neck where the Fermi surface touches the X faces. This orbit should be seen when the magnetic field is along a {110} direction; orientation is probably very critical.

β—a hole orbit around the sections that lie along the long sides of the X faces. These sections should give closed orbits even at a fairly large angle from the axis of the section.

τ—a hole orbit, coming out through the opening at the center of a T face, across the T face and X arm to the opening in the center of the X arm, and back to the center of the T face. The minimum area of this orbit corresponds to a magnetic field in the binary direction and the orbit is closed for a small angular range about this direction.

γ—a hole orbit, across the T face, from the hole in the center to the edge near W, through the opening in the L face, and back to the hole at the center of the T face. The minimum area corresponds to a magnetic field along the bisectrix direction (for a magnetic field rotating in the binary-bisectrix plane) and the orbit remains closed for a small angular range about this direction.

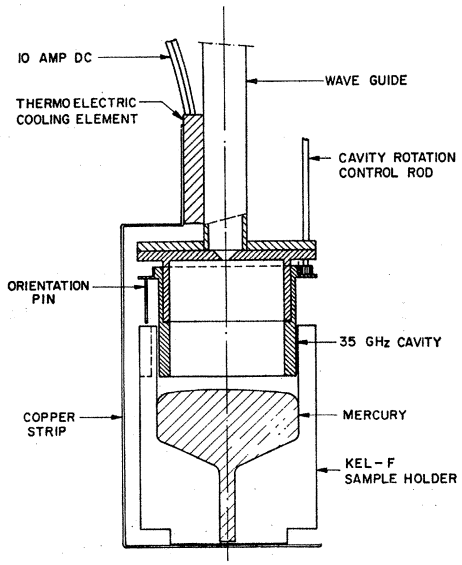

FIG. 4. The 35-GHz cavity and crystal-growing arrangement.

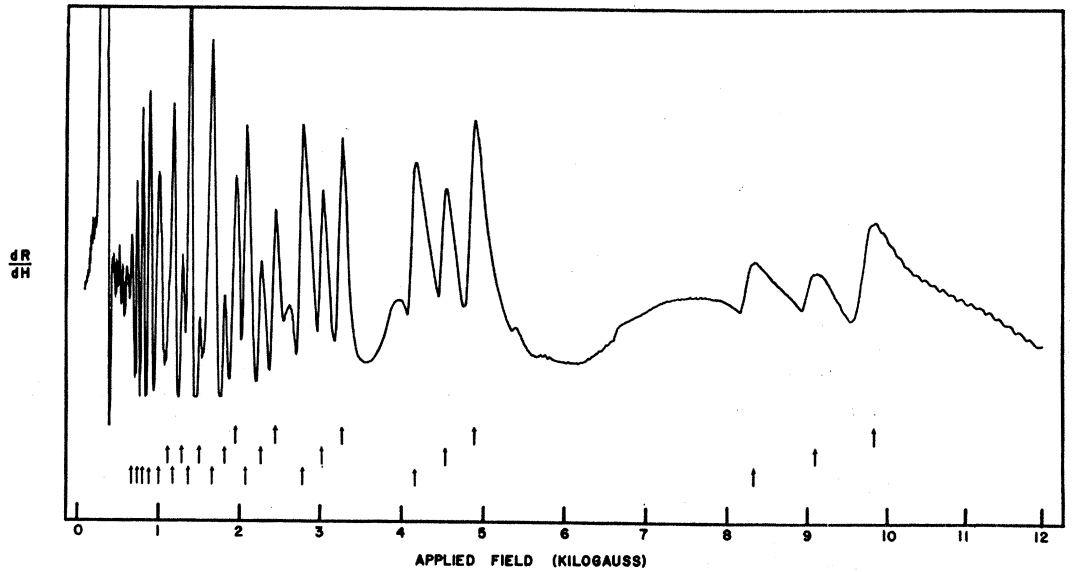

FIG. 5. Cyclotron resonance trace showing resonances from three groups of electrons taken with a microwave frequency of 34.9 GHz at 1.2°K for a magnetic-field direction of $32\frac{1}{2}°$ in Fig. 6.

μ—a hole orbit, stretching from the opening at the center of an X face, across the T face, to the opening at the center of another X face. The orbit is closed when the magnetic field is along the bisectrix direction and for a small angular range about this direction. When the magnetic field is rotated in the binary-bisectrix plane, the orbit has a minimum area at the bisectrix direction, and remains closed for a small angular range about this direction, the angular range depending on the size of the X-face necks.

de Haas–van Alphen oscillations of minimum frequency $f(H^{-1})=7.2\times10^5$ G, observed by Shoenberg,[3] showed that mercury had a small, anisotropic section on its Fermi surface. From a study of the resistivity of mercury, Ziman[14] concluded that the area of the Fermi surface of mercury was a little less than half the area of the free-electron Fermi sphere. Gustafson, Mackintosh, and Zaffarano,[4] in a positron-annihilation experiment, compared the angular distribution of photon coincidences from liquid and solid mercury. The plot for the solid could be fitted very well by a parabola corresponding to two free electrons per atom, indicating that the Fermi surface in extended k space did not depart significantly from a sphere. Brandt and Rayne,[15] using a de Haas–van Alphen effect torque magnetometer, measured the cross-sectional area of the β orbit and found it to have a minimum area of 0.0070 Å^{-2}, at a frequency corresponding closely to the frequency measured earlier by Shoenberg.[3] Their crystals were oriented using back-reflection Laué techniques. More recently, Brandt and Rayne[5] have discovered two other sets of oscillations, corresponding to the electron lenses (the α orbits) and to the τ orbits. Their measurements were made from 10 to 60 kG, using both a torque magnetometer and an rf technique. They obtained the effective mass of the β oscillations from the temperature variation of the amplitude of the torque oscillations between 1.1 and 4.2°K, obtaining a minimum of $0.12m_0$ and a maximum of $0.25m_0$. The effective mass of the τ oscillations was found to be between 0.9 and $1.1m_0$ with H parallel to $[10\bar{1}]$. From the rate at which the α oscillations decreased with temperature they concluded that the effective mass at the minimum area of the α oscillations was somewhat higher than that of the τ oscillations.

III. EXPERIMENTAL

Mercury crystals were grown *in situ*, using a thermoelectric device to provide a temperature gradient during crystal growth. The starting material was 99.99999% pure mercury, supplied by the United Mineral and Chemical Corp. of New York. The crystals were grown in a holder machined from Kel-F, which could be pulled up after growth was completed to make the free surface at the top of the mercury crystal the bottom of the microwave cavity.[15a] A thermoelectric device was used to maintain a temperature gradient in the mercury during crystal growth. After the experiment, a crystal was removed and stored for future use in a liquid-nitrogen Dewar. The 8-mm cavity and crystal-growing arrangement are shown in Fig. 4. Samples were oriented using back-reflection Laué photographs after the resonance experiments. Different sample orientations were obtained using different growth geometries, without

[14] J. M. Ziman, *Electrons and Phonons* (Oxford University Press, London, 1960), p. 374.
[15] G. B. Brandt and J. A. Rayne, Phys. Letters 15, 18 (1965).

[15a] Kel-F was chosen because its thermal expansion coefficient is relatively close to that of mercury.

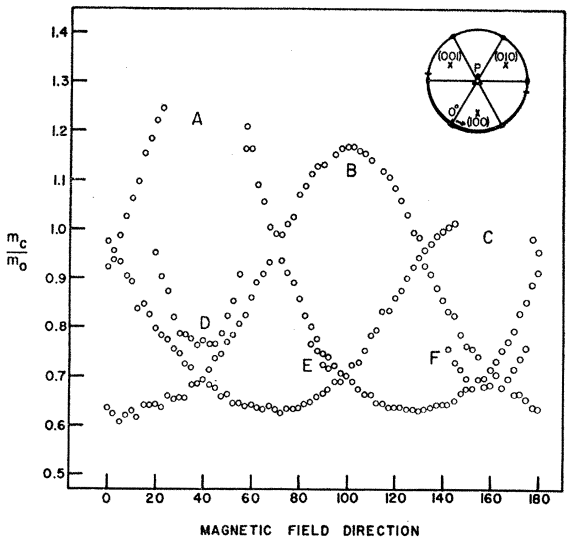

FIG. 6. Cyclotron effective-mass results for a sample surface oriented near the trigonal plane. Orientation is shown in the stereogram. The dot labeled P is the pole of the sample surface, situated at 4°±1° N, ½°±1° E; the straight lines, ending in the lenticular symbol, are binary axes. The direction labeled 0° is 8° from the projection of the nearest binary axis on the sample plane, and the sense of increasing angle is shown in the stereogram.

seeding. The methods used to grow and orient these crystals have been described fully in a previous paper.[16]

A 35-GHz Varian Spectrometer (model V-4503) was used for most of the measurements. Some measurements were also made with a 70-GHz spectrometer that has been described.[17] The microwave cavities resonated in a TE_{113} mode; the 35-GHz cavity is shown in Fig. 4, and was split so that it could be rotated about the axis of the cavity. A pin shown at the left side of the cavity slid into a slot in the sample holder, and oriented the sample surface with respect to the microwave cavity. The thermoelectric device is shown above the cavity to the left of the waveguide, with a copper cooling fin extending from it to below the sample. Most of the measurements were made with the microwave electric field at the sample surface polarized perpendicular to the magnetic field direction; some measurements were made with parallel polarization. Magnetic field strength was measured using a Rawson rotating-coil gaussmeter, accurate to 0.1%, that was calibrated by NMR. The magnetic field was supplied by a conventional 12-in. electromagnet that produced fields up to 20 kG. A vacuum pump was used to lower the temperature of the helium reservoir during experiments from 4.2 to 1.2°K.

The curvature of one of the sample surfaces was determined using a probe mounted on a travelling microscope stand that had vernier scales for both horizontal and vertical motion. An electrical circuit

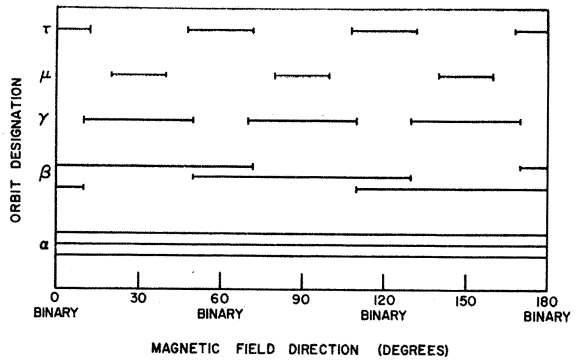

FIG. 7. Angular range over which orbits remain closed for magnetic-field directions in the trigonal plane.

was used to indicate when the probe was in contact with the sample. The shape was approximately spherical, with a radius of curvature of 27½ mm±10%. A section 8 mm in diameter formed the bottom of the cavity.

A cyclotron resonance trace showing Azbel'-Kaner resonance from three groups of electrons is shown in Fig. 5; subharmonic sets are indicated by three rows of arrows. Quantum oscillations of the microwave surface impedance that have been reported[18] are present above 10 kG. The large peak at 300–400 G, which saturated the spectrometer, is caused by the superconducting transition of the mercury sample. Subsidiary maxima on the low-field side of some of the subharmonics are attributed to the slightly curved sample surface. The small peaks at 3.95 and 2.61 kG are examples of these subsidiary maxima. If these peaks are plotted on a graph of $1/H$ versus the subharmonic number n, they yield a straight line that crosses the n axis at about $n=-0.5$, whereas a plot of the large peaks yields a straight line that crosses the n axis between $n=\pm 0.05$. This value at the intercept is called the zero shift of the resonance. The small peak at 5.39 kG was observed in many traces, falling between 4.5 and 6.0 kG depending on the direction of the magnetic field. Its origin cannot be explained at this time. The small increase in dR/dH at 6.60 kG was caused by changing the time constant of the spectrometer from $\frac{1}{10}$ to 1 sec.

Measurements were made at both 35 and 70 GHz, and the anisotropy of the cyclotron effective mass was plotted for a range of magnetic field directions of 180° in the sample plane. The cyclotron effective mass and the zero shift were calculated from the data using a least-squares computer program to fit the best straight line to a plot of $1/H_n$ versus n, where H_n were values of magnetic field at derivative-signal maxima. The cyclotron mass was calculated from $m_c^*=e/\omega cs$, where s is the slope of the line and ω is the microwave frequency.

[16] A. E. Dixon, J. S. Moss, and W. R. Datars, Mat. Res. Bull. 2, 595 (1967).
[17] W. R. Datars, Can. J. Phys. 40, 1784 (1962).
[18] R. G. Poulsen, A. E. Dixon, and W. R. Datars, Bull. Am. Phys. Soc. 12, 703 (1967).

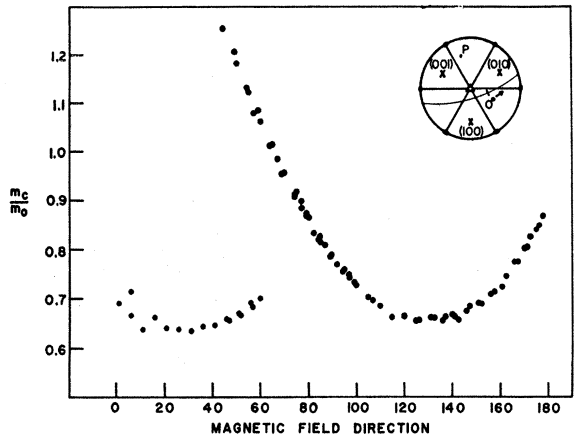

FIG. 8. Cyclotron effective-mass results at 69.6 GHz for the crystallographic plane shown in the stereogram. The pole of the sample surface is at 62½°±2° N, 36°±2° W, and the point labeled 0° is 57° from the intersection of the sample plane with the trigonal plane.

IV. CYCLOTRON MASSES AND THEIR INTERPRETATION

Figure 6 shows the cyclotron effective-mass results of an experiment at 34.9 GHz on a mercury crystal whose sample surface was tilted 4° from the trigonal plane. The orientation of the sample surface relative to the trigonal plane is shown in the stereogram in the top right corner of the figure. The position of the pole of the sample surface on the stereogram, in latitude and longitude, is 4°±1° N, ½°±1° E. The magnetic field direction labeled 0° on the graph is shown on the stereogram by a short straight line cutting the sample plane, and the direction of rotation of the magnetic field in the sample plane is indicated with an arrow. The possible cyclotron orbits for a magnetic field direction in the trigonal plane are shown in Fig. 2(b), with the exception of the α orbits around the second-zone electron lenses. The approximate angular range through which each of these orbits should be observed was estimated using a model based on the band-structure calculation of Keeton and Loucks[8] and is shown in Fig. 7.

Mass curves for the β, γ, and μ orbits are centered on bisectrix directions, while those of the τ orbits are centered on binary directions. Cyclotron-resonance signals from the three electron lenses are possible for any magnetic field direction, and the signal from a lens will indicate a maximum cyclotron effective mass for a magnetic field along one of the bisectrix directions and a minimum effective mass for a magnetic field along the binary direction perpendicular to that bisectrix direction. Mass curves A, B, and C of Fig. 6 are attributed to α orbits on electron lenses tiled 70°, 66°, and 63°, respectively, from the normal to the sample surface. The curves labeled D, E, and F are visible for an angular range of 35° and are centered on bisectrix directions. Curve D, which has the largest minimum mass, lies under curve A, which has the largest maximum mass of the three lenses. The Fermi-surface model (RAPW) predicts that, for the β and μ orbits, the curve with the smallest minimum mass should lie under A, which is not observed. For this reason, and because it is visible over almost the same angular range as that predicted for the γ orbit in Fig. 7, D, E, and F are attributed to γ orbits.

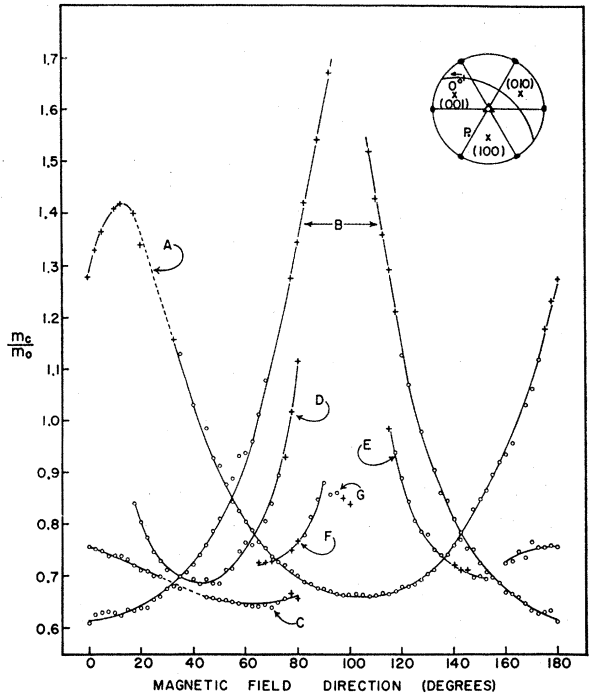

FIG. 9. Cyclotron effective-mass results from a sample oriented with the pole of the sample surface at 36°±1° S, 30°±1° W. The point labeled 0° is 27° from the intersection of the sample plane with the trigonal plane.

Results of an experiment at 69.6 GHz are shown in Fig. 8. The sample orientation is shown in the stereogram, where the pole of the sample surface is at 62½°±2° N, 36°±2° W. A Laué picture of the sample surface showed a (110) axis and a binary axis each 25° from the normal to the sample surface, and in the same plane as the normal. The long curve of mass values on the right of the diagram corresponds to an α orbit on an electron lens tilted 70° from the normal to the sample surface. The mass values on the left of Fig. 8 correspond to α orbits on the other two electron lenses. The agreement of cyclotron masses of the α orbits obtained from the 70-GHz data with those obtained from the 35-GHz data confirms that the oscillations observed are cyclotron-resonance oscillations. Similar but less precise results at 35 GHz were reported earlier[9] from a pair of samples oriented with two {100} directions in the plane of the sample surface. These results were originally attributed to the β orbits, when the data of Fig. 7 were not available. In that particular sample plane, the minimum mass of the β orbit is at the same

magnetic field direction as the minimum mass of the α orbit, and anisotropy of the two orbits are very similar near the minimum mass.

Figure 9 shows results at 34.8 GHz from a crystal oriented as shown in the stereogram. The pole of the sample surface was at 36°±1° S, 30°±1° W. Data points shown as open circles are from relatively strong signals, and were calculated using the least-squares computer program described in Sec. III. Data points shown as plus signs are from weak signals that resulted in only one derivative peak, usually the first subharmonic. In many cases it should have been possible to see more than one peak, but the subharmonics of a weak signal were often masked by the large subharmonics of one of the electron lenses. Mass curves A, B, and C are attributed to α orbits on the three electron lenses, tilted 70°, 72°, and 34°, respectively, from the plane of the sample surface. Curves D and E are attributed to γ orbits, by comparison with Fig. 6, and because they lie in the proper position for γ orbits in this plane. Curve F results from a weak set of signals that are attributed to the τ orbit, and the set of four very weak signals labeled G falls at exactly the proper position for the μ orbit, and is tentatively attributed to that orbit.

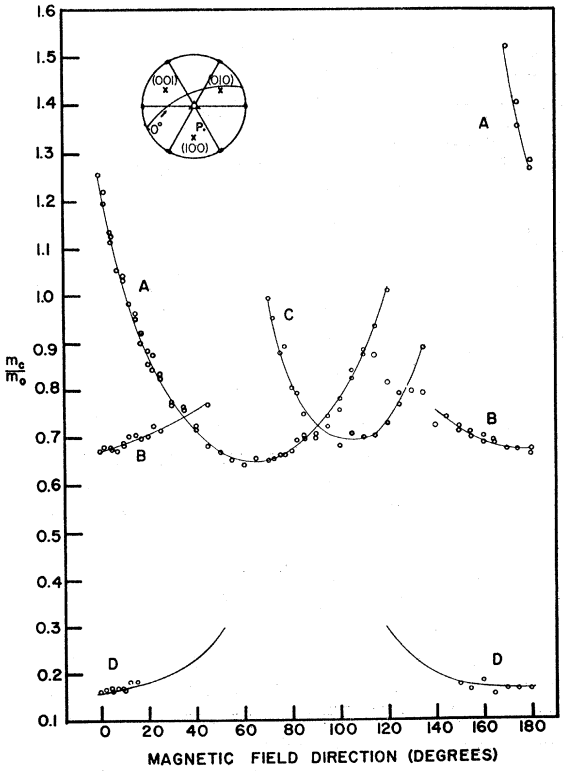

FIG. 10. Cyclotron effective-mass results from a sample oriented with the pole of the sample surface at 50°±2° S, 30°±2° E. The point labeled 0° is at the intersection of the sample plane and the trigonal plane. The curve drawn through the group of points marked D is a cylindrical fit.

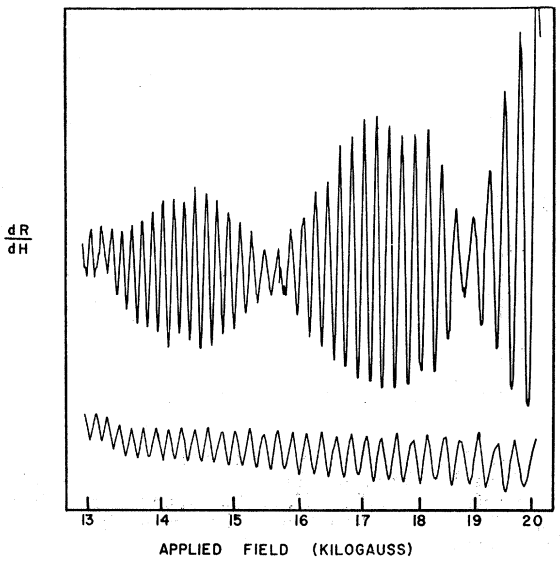

FIG. 11. Quantum oscillations of the microwave surface impedance.

The results of an experiment at 34.8 GHz are shown in Fig. 10. The sample orientation is shown in the stereogram, with the pole of the sample surface located at 50°±2° S, 30°±2° E. The mass curve labeled A is attributed to an α orbit on an electron lens tilted 82° from the normal to the sample surface. The curve labeled B is assigned to the α orbit on a second lens, tilted 70° from the normal to the sample surface. The mass curve C is attributed to a γ orbit, since it occurs for a range of magnetic field directions for which a γ orbit is possible and has a minimum-mass value close to that of the γ orbit in Fig. 6. Mass curve D, with a minimum mass of $0.16m_0$, is attributed to the β orbit. It is shown with a cylindrical fit superimposed. For this particular sample orientation, one of the β arms is oriented with the long dimension of its cross section perpendicular to the sample surface in reciprocal space, so that the real-space orbit of these electrons has its long dimension parallel to the sample surface. Signal strength at resonance is inversely proportional to the Gaussian curvature of the Fermi surface at that part of the reciprocal-space orbit that corresponds to the section of the real-space orbit lying inside the skin depth,[19] and in this case the curvature is small. Thus the observation of this β orbit is favored over other β orbits having larger Gaussian curvature. de Haas–van Alphen effect measurements have indicated an effective mass of $0.18m_0$ for the β orbit.[5] Measurements with the microwave electric field parallel to the dc magnetic field resulted in large cyclotron-resonance signals from the α orbits on the electron lenses, but no signals from other orbits were observed in this configuration.

[19] A. B. Pippard, Rept. Progr. Phys. 23, 176 (1960).

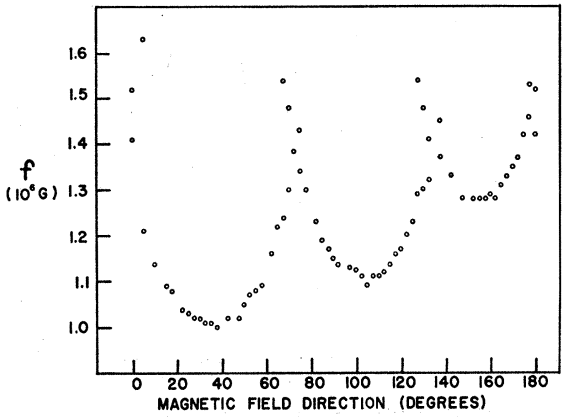

FIG. 12. Frequencies of quantum oscillations observed in the sample whose orientation is shown in Fig. 6.

V. QUANTUM OSCILLATIONS OF MICROWAVE SURFACE IMPEDANCE

Oscillations of the microwave surface impedance for magnetic field strengths above 10 kG have been observed during cyclotron-resonance experiments at 1.2°K. Examples of these oscillations are shown in Fig. 11. The top curve shows beating of two frequencies near a crossover point of the data of Fig. 12. The bottom curve is typical of the results obtained from this sample (cyclotron-resonance results for this sample are shown in Fig. 6). The oscillations are periodic in $1/H$, and if analyzed as cyclotron-resonance subharmonics yield an effective mass much larger than would be expected in mercury. If the oscillations are analyzed in the same way as de Haas–van Alphen oscillations, they yield results identical in both frequency and anisotropy to de Haas–van Alphen results from the β orbits.[5] For this reason, the oscillations are identified as quantum oscillations of the microwave surface impedance. A plot of the frequencies observed is shown in Fig. 12, where the sample orientation is the same as that for the cyclotron-resonance results in Fig. 6. The angular range over which each branch is observed is just a little smaller than that predicted for the β orbit in Fig. 7, and larger than the angular range of either the γ or μ orbits, which are also centered on bisectrix axes. In Fig. 12, the two data points at the top left of the diagram are part of the data curve on the right, and two of the data points at top right are part of the data curve on the left. No frequencies corresponding to any other orbit were observed. A study of the shape of β arms is being made, utilizing large tilt angles of the magnetic field from the sample surface.[18]

[20] J. F. Koch, R. A. Stradling, and A. F. Kip, Phys. Rev. 133, A240 (1964).
[21] D. N. Langenberg and S. M. Marcus, Phys. Rev. 136, A1383 (1964).
[22] C. C. Grimes and A. F. Kip, Phys. Rev. 132, 1991 (1963).
[23] F. W. Spong and A. F. Kip, Phys. Rev. 137, A431 (1965).

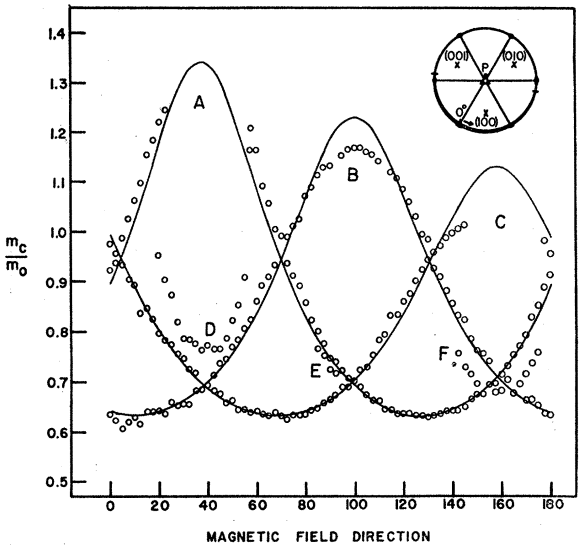

FIG. 13. Ellipsoidal fit to cyclotron masses of the electron lenses.

VI. DISCUSSION OF EXPERIMENTAL RESULTS

A. Effects of Curved Sample Surface on Cyclotron-Resonance Signals

The subsidiary maxima on the low-field side of the cyclotron-resonance derivative signals (see Fig. 5) were attributed to the effects of a slightly curved sample surface. The effects of small-angle tipping of the sample surface with respect to the dc magnetic field have been discussed by several investigators (Koch, Stradling, and Kip[20]; Langenberg and Marcus[21]; Grimes and Kip[22]; and Spong and Kip[23]). None of the explanations of the effect is completely satisfactory in explaining the results observed in mercury because the mercury sample surfaces were curved rather than having flat surfaces tilted with respect to the magnetic field direction. A full explanation is not proposed. However, the curved surfaces may introduce an error in the cyclotron effective-mass values. In other experiments the change in mass values due to the tilt of the magnetic field to the sample surface was accompanied by a large zero shift in the plot of $1/H_n$ versus the subharmonic number n. The zero shift in this experiment is of the order of $<\pm 0.05$, so that the mass shift caused by the curved surface is expected to be small. An estimate of the mass shift can be obtained by tilting the magnetic field from a sample with a flat surface. Preliminary results with the magnetic field parallel to a flat mercury surface showed no subsidiary maxima, and tipping of the magnetic field from the surface indicated a mass shift for the α orbits that was less than 3% for a tilt of 1°.

B. Cyclotron-Resonance Masses

A least-squares fit has been made to the data from one of the second-zone electron lenses, to compare the

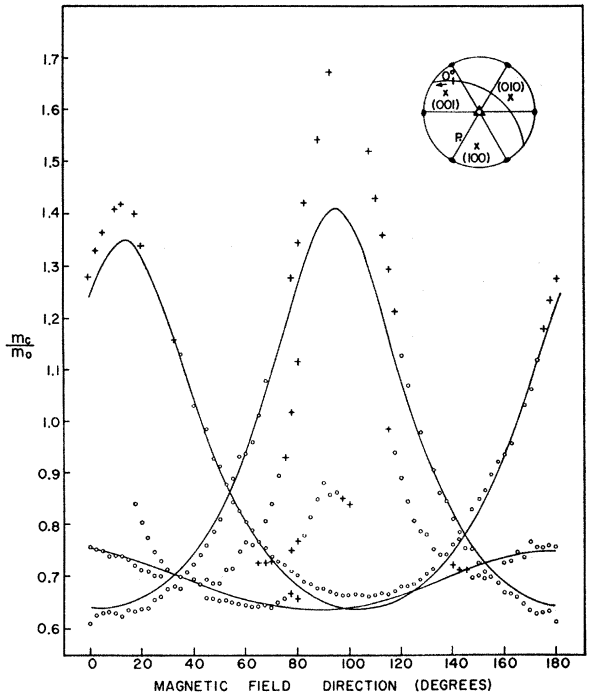

FIG. 14. Comparison of the predictions of the ellipsoidal approximation of the electron lenses with the data of Fig. 9.

lens with an ellipsoid of revolution. An expression for the cyclotron effective mass for an ellipsoidal energy surface[24] in a magnetic field with direction cosines α, β, and γ with respect to the principal axes of the ellipsoid is given by

$$m_c^*=\left(\frac{m_1m_2m_3}{m_1\alpha^2+m_2\beta^2+m_3\gamma^2}\right)^{1/2}.$$

This can be written in terms of the variables $\sin^2\theta$ and $\cos^2\theta$:

$$\frac{1}{m^{*2}}=\frac{1}{m_2m_3}\sin^2\theta+\left(\frac{\cos^2K}{m_1m_3}+\frac{\sin^2K}{m_1m_2}\right)\cos^2\theta,$$

where K is the angle between the major axis of the ellipsoid and the normal to the sample surface and θ is an angle in the plane of the sample surface, measured from the projection of the major axis of the ellipsoid on the plane of the sample surface to the magnetic field direction.

The data of curve B in Fig. 6 were fitted with an ellipsoid of revolution, and the results of this calculation were compared with the data from other second-zone electron lenses. The lens of curve B was tilted 66°±1° from the normal to the sample surface. The parameters of the ellipsoid of revolution that best fit the data were $m_1=m_2=0.219m_0$ and $m_3=1.84m_0$. The fit is not adequate at high masses, indicating that the

[24] W. Shockley, Phys. Rev. **90**, 491 (1953).

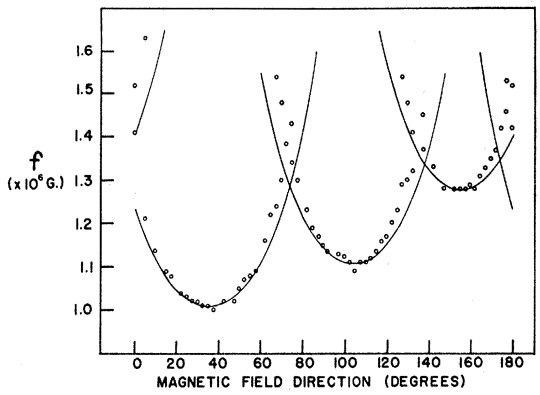

FIG. 15. Cylindrical fit to the quantum-oscillation data.

lens is not an ellipsoid of revolution, but it does not indicate where the deviation takes place, since the least-squares fit tries to fit the low-mass values because of the large number of points there. These parameters were then used to fit lens A (tilt angle 70°±1°) and lens C (tilt angle 63°±1°). The results of these comparisons are shown in Fig. 13. The best fit for lens C was for a tilt angle of 62°; this is the comparison shown in Fig. 13.

The adequacy of the model can be tested by using a second plane giving different cross sections of the lenses. The parameters from the fit of curve B in Fig. 6 were used to fit the data of Fig. 9 as shown in Fig. 14. The fit is poor at both low- and high-mass values, indicating that the lenses are not a surface of revolution and may have the shape shown in Fig. 3. A measurement of the effective mass for all magnetic field directions around a lens whose major axis is normal to the sample surface would be useful to show how far the lens differed from a surface of revolution. The latter would give a constant effective mass for a lens having this orientation. Experimentally, this is a difficult problem, because the Gaussian curvature of the section of the lens orbit inside the skin depth is large for a lens with this orientation, resulting in low signal strength. At the same time, the other two lenses have orientations such that they give large signals and tend to mask signals from the third lens.

Of the cyclotron orbits observed in this experiment only the α orbit is present in a similar form in the single-OPW approximation. This approximation predicts a minimum cyclotron effective mass for the α orbit (electron lens) of $0.36m_0$ and a maximum mass of $1.0m_0$. This experiment has measured a minimum effective mass for the α orbit of from $0.60m_0$ to $0.66m_0$, depending on the orientation of the lens relative to the sample plane. The maximum mass has not been measured, but it can be estimated from Fig. 9 to be about $1.75m_0$. The discrepancy between the measured and predicted values is of the same order of magnitude as that found by Harrison[13] in aluminum and is partially due to the fact that electron-electron and electron-phonon interactions

are not included in the single-OPW mass. The effect of the electron-electron interaction on the effective mass of electrons in polyvalent metals is expected to be small[25] but the electron-phonon interaction may considerably enhance the band-structure mass.[26]

An orbit that stretches across the top face of the Brillouin zone in the single-OPW approximation, from W, through T, and across to the opposite corner in Fig. 1, would be cut in two by the existence of a neck through the T face. Then, using this approximation, the cyclotron mass of the γ orbit is predicted to be $0.40m_0$; this experiment measures an effective mass of $0.7m_0$ (see Fig. 6), with the magnetic field along a bisectrix direction. Because the single-OPW approximation normally predicts a mass that is too small, and because the orbit is observed over a larger angular range than would be expected for the single-OPW orbit, these data are taken as evidence for a neck through the T face of the Brillouin zone, resulting in the γ orbit shown in Fig. 2(b). If a mass value equal to half that predicted by the single-OPW approximation is used for the γ orbit, then the mass ratio (ratio of the measured cyclotron effective mass to that predicted by the single-OPW approximation), for both the α and γ orbits, lies within the range 1.75 ± 0.1.

The β orbit, shown in Fig. 2(b), has a cross-sectional area (measured from the quantum-oscillation data) of $\frac{1}{10}$ of the area of the same orbit in the single-OPW approximation, suggesting that contact of the Fermi surface at the center of the X faces has broken the single-OPW arm into two narrow tubes directed along the long dimension of the X faces. The existence of an area of contact of the Fermi surface with the Brillouin zone at both the X and T faces has been noted previously in both de Haas–van Alphen[5,15] and magnetoresistance studies.[6,7] The μ and τ orbits, also shown in Fig. 2(b), depend for their existence on the areas of contact of the Fermi surface with the T and X faces, and there are no analogous orbits in the single-OPW model. The RAPW model[8] predicts areas of contact at the centers of the T and X faces, and was used to estimate the angular range through which the various cyclotron orbits remained closed (see Fig. 7).

[25] T. M. Rice, Ann. Phys. (N. Y.) **31**, 100 (1965).
[26] N. W. Ashcroft and J. W. Wilkins, Phys. Letters **14**, 285 (1965).

C. Cylindrical Fit to Quantum-Oscillation Data

The cross-sectional area of a cylinder at an angle θ from the minimum cross-sectional area in the plane of rotation of the magnetic field direction is $A(\theta)=A_0/\cos\theta$, where A_0 is the minimum area of the cylinder in that plane. Since the frequency of the oscillations is proportional to A, then $f(\theta)=f_0/\cos\theta$. A cylindrical fit to the quantum-oscillation data is shown in Fig. 15, where f_0 was taken to be the minimum frequency in each branch. The fitted curve in each case lies outside the experimental curve as θ is increased, showing that the cross-sectional area of this orbit increases faster than that for a cylinder. The experimental result represents a cylinder that is flared out at the ends where it joins the rest of the Fermi surface.

VII. CONCLUSIONS

Cyclotron-resonance signals with as many as 20 subharmonics have been observed in single-crystal mercury. Experiments were performed on crystals with slightly curved sample surfaces, causing some distortion of the cyclotron-resonance derivative signals. The mass shift caused by these distortions was probably small. The results may be interpreted using predictions of the Keeton-Loucks model of the Fermi surface. The minimum cyclotron effective mass of the α orbits (electron lenses) is $0.63m_0$, for a magnetic field along the binary direction. An ellipsoidal fit to the cyclotron effective-mass data from the electron lenses shows that they deviate from an ellipsoidal shape when approximated by an ellipsoid of revolution with parameters $m_1=m_2=0.219m_0$, and $m_3=1.84m_0$. The minimum cyclotron effective mass of the γ orbit in the trigonal plane is $0.69m_0$; the minimum mass of the β orbit is $0.16m_0$. A weak set of signals of minimum mass $0.72m_0$ is attributed to the τ orbit. The ratio of the measured cyclotron effective mass to that predicted by the single-OPW approximation for both α and γ orbits is 1.75 ± 0.1. There are oscillations of the microwave surface impedance above 10 kG that are quantum oscillations from the β arms of the Fermi surface.

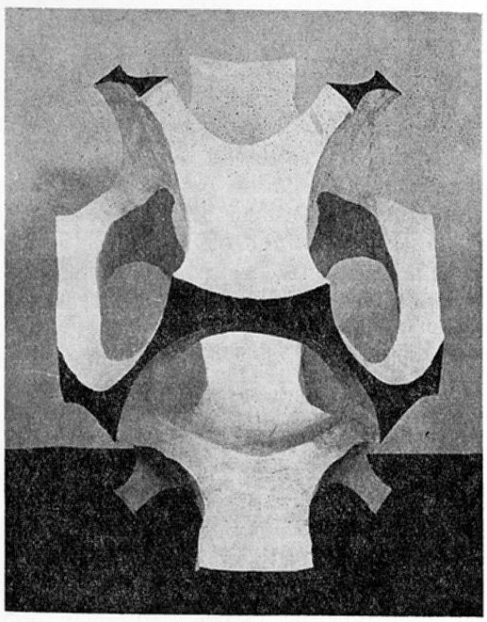

(a)

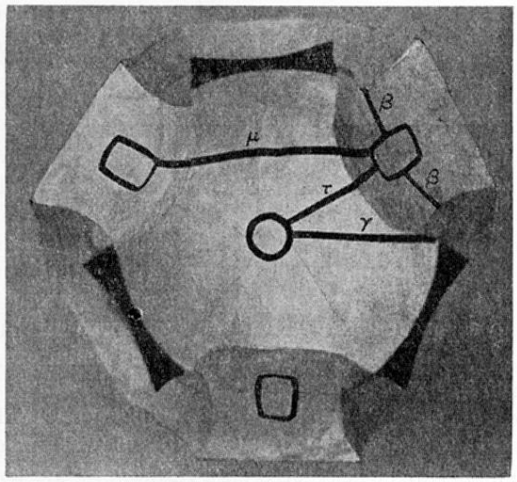

(b)

FIG. 2. (a) Model of the first-zone single-OPW surface of mercury. (b) Some of the closed orbits possible if the Fermi surface touches the zone boundary at the center of the T and X faces of the Brillouin zone.